



**HAL**  
open science

# An information-theoretic framework for optimal design: analysis of protocols for estimating soft tissue parameters in biaxial experiments

Ankush Aggarwal, Damiano Lombardi, Sanjay Pant

## ► To cite this version:

Ankush Aggarwal, Damiano Lombardi, Sanjay Pant. An information-theoretic framework for optimal design: analysis of protocols for estimating soft tissue parameters in biaxial experiments. *Axioms*, 2021. hal-03187110

**HAL Id: hal-03187110**

**<https://inria.hal.science/hal-03187110>**

Submitted on 31 Mar 2021

**HAL** is a multi-disciplinary open access archive for the deposit and dissemination of scientific research documents, whether they are published or not. The documents may come from teaching and research institutions in France or abroad, or from public or private research centers.

L'archive ouverte pluridisciplinaire **HAL**, est destinée au dépôt et à la diffusion de documents scientifiques de niveau recherche, publiés ou non, émanant des établissements d'enseignement et de recherche français ou étrangers, des laboratoires publics ou privés.

# An information-theoretic framework for optimal design: analysis of protocols for estimating soft tissue parameters in biaxial experiments

Ankush Aggarwal <sup>1,†</sup> , Damiano Lombardi <sup>2,†</sup>  and Sanjay Pant <sup>3,†,\*</sup> 

<sup>1</sup> Glasgow Computational Engineering Centre, James Watt School of Engineering, University of Glasgow, Glasgow, UK

<sup>2</sup> Centre de Recherche INRIA de Paris & Laboratoire Jacques-Louis Lions, France

<sup>3</sup> Zienkiewicz Centre for Computational Engineering, College of Engineering, Swansea University, Swansea, UK

\* Correspondence: Sanjay.Pant@swansea.ac.uk

† These authors contributed equally to this work.

**Abstract:** A new framework for optimal design based on the information-theoretic measures of mutual information, conditional mutual information, and their combination is proposed. The framework is tested on the analysis of protocols—combination of angles along which strain measurements can be acquired—in a biaxial experiment of soft tissues for the estimation of hyperelastic constitutive model parameters. The proposed framework sees information gain about the parameters from the experiment as the key criterion to be maximised which can be directly used for optimal design. Information gain is computed through  $k$ -nearest neighbour algorithms applied to the joint samples of the parameters and measurements produced by the forward and observation models. For biaxial experiments, the results show that low angles have relatively low information content compared to high angles. They also show that fewer number of angles with suitably chosen combinations can result in higher information gains when compared to a larger number of angles which are poorly combined. Finally, it is shown that the proposed framework is consistent with classical approaches, particularly the D-optimal design.

**Citation:** Aggarwal, A.; Lombardi, D.; Pant, S. An information-theoretic framework for optimal design: analysis of protocols for estimating soft tissue parameters in biaxial experiments. *Axioms* **2021**, *1*, 0. <https://doi.org/>

Received:

Accepted:

Published:

**Publisher's Note:** MDPI stays neutral with regard to jurisdictional claims in published maps and institutional affiliations.

**Copyright:** © 2021 by the authors. Submitted to *Axioms* for possible open access publication under the terms and conditions of the Creative Commons Attribution (CC BY) license (<https://creativecommons.org/licenses/by/4.0/>).

**Keywords:** optimal design; soft tissue mechanics; mutual information; biaxial experiment; inverse problems; information theory.

## 1. Introduction

Soft tissues exhibit complex biomechanical behaviour, including nonlinearity, anisotropy and heterogeneity [1]. Moreover, the tissues also demonstrate inelastic properties, such as rate-dependence, hysteresis and permanent set. The important link between the biomechanics and their physiological function have motivated a large number of ex-vivo studies aimed at characterizing their biomechanical properties. Given the complex interplay between the different aspects of their biomechanical properties, the experimental design of ex-vivo soft tissues is extremely challenging and has been a subject of investigation with a variety of experiments been proposed [2–6].

Since a variety of soft tissues are thin, e.g., blood vessels, heart valves and skin, biaxial testing is a widely used experimental technique that allows independently stretching the tissue in two orthogonal directions and measuring the corresponding forces [7,8]. Applying different stretches in two directions allows characterization of the in-plane anisotropic behavior of a given tissue, while a range of stretches provides us its nonlinear elastic response. However, even with this relatively simple set of options, the choices of what stretches to apply are unclear. Moreover, it is not obvious what these choices will depend on.

33 A variety of hyperelastic models have been developed to describe the anisotropic  
 34 and nonlinear elastic properties of specific soft tissues [4,9–11]. The biaxial experimental  
 35 data is commonly fit to these models in order to determine the model parameters. As the  
 36 unknown parameters depend on specific model, the choice of experimental setup—the  
 37 problem of optimal design—might depend on the choice of model. However, in practice,  
 38 a predetermined set of experimental protocols are used.

39 In the present work, an optimal design problem is defined as finding the most  
 40 suitable protocol in view of estimating the parameters of the material model. A compre-  
 41 hensive overview of the optimal design problem can be found in [12,13], and several  
 42 criteria for optimal design have been proposed in the literature, often based on the  
 43 minimisation of the variance of the parameters and sensitivities [14,15]. In the present  
 44 work, we investigate a criterion based on information theoretic quantities, in the spirit of  
 45 what has been proposed in the work [16] (from a Bayesian point of view) and [17]. The  
 46 goal is to characterise the amount of information the measurements convey about the  
 47 parameters we would like to estimate and then maximise that information. Estimating  
 48 information theoretic quantities is in general a challenging problem, and this is especially  
 49 the case in high-dimensional settings. In the present work, a model reduction method is  
 50 coupled with a non-parametric sample based mutual information estimation in order to  
 51 provide a pertinent estimation of the information theoretic quantities involved in the  
 52 optimal design problem and then applied to the biaxial testing of soft tissues.

53 The structure of the work is as follows: in Section 2 the model and information the-  
 54 oretical aspects of the problem are introduced. In particular, in Section 2.1 we detail the  
 55 mathematical model of the biaxial experiments for soft tissues: after having introduced  
 56 the notation and the non-linear elasticity model, in Section 2.1.1 we particularise it to  
 57 the biaxial testing experimental setup. In Section 2.1.2 we introduce the experimental  
 58 protocol definition.

59 The second part of the Section is devoted to the description of the information-  
 60 theoretic framework for solving the optimal design problem. In Section 2.2.1 we intro-  
 61 duce the problem, in Sections 2.2.2 and 2.2.3 the information-theoretic quantities and  
 62 their numerical estimation are detailed. We then present the reduce order modeling  
 63 method used and how to validate the results obtained by the proposed approach. The  
 64 section ends with an overview of the method.

65 The results and the discussion are presented in Section 3, followed by the conclusion  
 66 and the perspectives.

## 67 2. Methods

68 The methodological aspects are divided into two broad categories: the mathemat-  
 69 ical model of the biaxial experiments; and the information-theoretic optimal design  
 70 framework.

### 71 2.1. Mathematical model of the biaxial experiments

72 We begin by defining the notation: a material point at its reference position  $\mathbf{X} \in \mathbb{R}^3$   
 73 moves to  $\mathbf{x} \in \mathbb{R}^3$  after deformation. The elastic behavior of soft tissues is described using  
 74 hyperelastic strain energy density  $\Psi$  which depends on the deformation gradient tensor  
 75  $\mathbf{F} = \nabla_{\mathbf{X}}\mathbf{x}$ . The ratio of volume after deformation to that before deformation is given by  
 76  $J = \det(\mathbf{F})$ . Soft tissues are commonly regarded as incompressible due to high water  
 77 content, i.e.  $J$  is constrained to be unity.

78 We consider the hyperelastic model proposed by Gasser et al.[18] which defines the  
 79 strain energy density

$$\Psi = \frac{k_1}{2k_2} \left[ e^{k_2(\kappa I_1 + (1-3\kappa)I_4 - 1)} - 1 \right] + \mu(I_1 - 3), \quad (1)$$

80 where  $I_1 = \text{tr}(\mathbf{F}^\top \mathbf{F})$  is the first invariant of the right Cauchy-Green strain tensor  $\mathbf{C} = \mathbf{F}^\top \mathbf{F}$   
 81 and  $I_4 = \mathbf{M} \cdot \mathbf{C} \mathbf{M}$  is the fourth invariant representing stretch along fiber direction  $\mathbf{M}$ .  
 82 The resulting Cauchy stress is given by

$$\sigma = 2\mathbf{F} \cdot \frac{\partial \Psi}{\partial \mathbf{C}} \cdot \mathbf{F}^\top - p\mathbf{I}, \quad (2)$$

83 where  $p$  acts as the Lagrange multiplier to enforce incompressibility and  $\mathbf{I}$  is the identity  
 84 matrix.

85 For this model, the set of unknown parameters can be written as  $\{k_1, k_2, \kappa, \mu\}$   
 86 assuming that the fiber direction  $\mathbf{M}$  is known a priori (based on another experiment,  
 87 e.g., light scattering [6]). In this paper, in order to simplify the problem, we assume that  
 88  $\kappa = 0.1$  and  $\mu = 0.1$  kPa are known and fixed. Thus, the aim of an ex-vivo biomechanical  
 89 experiment is to determine parameters  $k_1 \in [5, 100]$  kPa and  $k_2 \in [5, 80]$  robustly and  
 90 with high confidence [19,20]. A commonly used experiment called the biaxial testing is  
 91 described next.

### 92 2.1.1. Biaxial experiments for soft-tissues

93 Many of the soft tissue types are planar with small thickness. In a biaxial experiment,  
 94 a square-shaped tissue sample is mounted via clamps or rakes and stretched along two  
 95 orthogonal directions aligned with the sample edges (Fig. 1a). If these directions are  
 96 used as the two coordinate axes and incompressibility is assumed, the stretching results  
 97 in a diagonal deformation gradient tensor

$$\mathbf{F} = \text{diag} \left[ \lambda_1, \lambda_2, \frac{1}{\lambda_1 \lambda_2} \right], \quad (3)$$

98 where  $\lambda_1$  is the stretch along first in-plane direction and  $\lambda_2$  is the stretch along  
 99 second in-plane direction. The fiber direction  $\mathbf{M}$  is generally aligned with the first  
 100 coordinate axis, which results in only normal stress components. As no force is applied  
 101 along the thickness of the tissue,  $\sigma_{33} = 0$  is used to determine the Lagrange multiplier  $p$ .  
 102 Thus, we get

$$\sigma_{11} = 2 \frac{\partial \Psi}{\partial I_1} \left[ \lambda_1^2 - \frac{1}{\lambda_1^2 \lambda_2^2} \right] + 2 \frac{\partial \Psi}{\partial I_4} \lambda_1^2 \quad (4)$$

$$\sigma_{22} = 2 \frac{\partial \Psi}{\partial I_1} \left[ \lambda_2^2 - \frac{1}{\lambda_1^2 \lambda_2^2} \right]. \quad (5)$$

103 The applied stresses  $\sigma_{11}, \sigma_{22}$  are controlled using load cells. The resulting strains defined  
 104 as  $e_1 := \lambda_1 - 1$  and  $e_2 := \lambda_2 - 1$  are measured from the marker positions<sup>1</sup>. It is important  
 105 to note that a homogeneous stress and strain state is assumed in the middle of the sample  
 106 (Fig. 1a). Therefore, an implicit assumption is that the material properties and sample  
 107 thickness are homogeneous. Moreover, these measurement techniques carry an error  
 108 due to the limitations in measurement tools and/or the deviation from homogeneity,  
 109 incompressibility and material direction.

### 110 2.1.2. Protocol definition

111 In practice, there are two approaches to the biaxial experiment: 1) displacement  
 112 controlled where known stretches are imposed and forces are measured and 2) force  
 113 controlled where known forces are applied and stretches are measured. Generally, the  
 114 force controlled approach is used as it is easier to implement. Therefore, in the force  
 115 controlled approach, different values of stresses  $\sigma_{11}$  and  $\sigma_{22}$  can be applied.

<sup>1</sup> Although  $e_1$  and  $e_2$  are not the usual strain measures, we use these as our observations

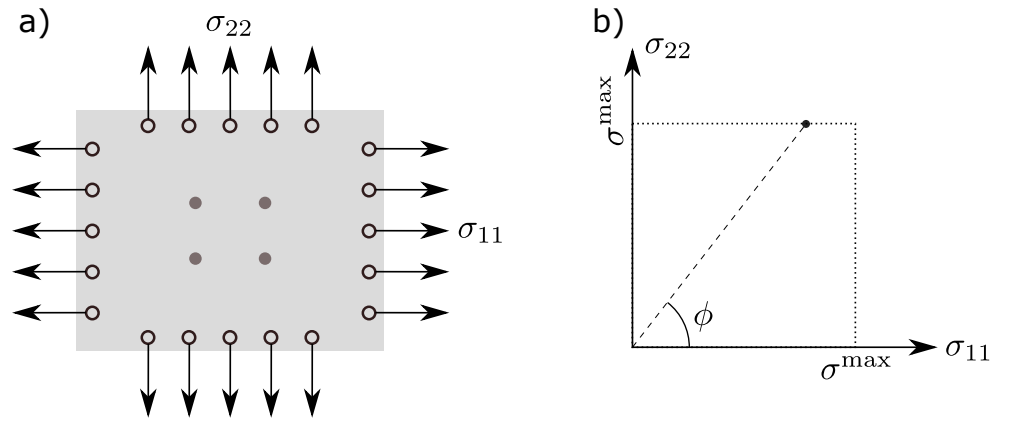


**Figure 1.** a) A schematic of a biaxial experimental setup where a thin planar tissue sample (in light gray) is mounted via rakes and two orthogonal forces are applied to induce stresses  $\sigma_{11}$  and  $\sigma_{22}$ , and the resulting strains are measured by tracking the locations of the markers (in dark gray). b) The  $\sigma_{11} - \sigma_{22}$  space, where the applied stresses lie on the dotted line with a finite number of protocol angles  $\phi$  used.

116 A single-angle biaxial protocol is defined as a straight line in the  $\sigma_{11} - \sigma_{22}$  space (Fig.  
 117 1b). That is, the ratio between the two stresses is kept constant while the applied forces  
 118 are increased until a maximum value  $\sigma^{\max} = 200$  kPa. Thus, for a chosen angle  $\phi$ , we  
 119 apply:

$$\sigma_{11} = \begin{cases} \sigma & \text{if } \phi \leq \frac{\pi}{4} \\ \tan(\phi)\sigma & \text{else} \end{cases} \quad (6)$$

$$\sigma_{22} = \begin{cases} \cot(\phi)\sigma & \text{if } \phi \leq \frac{\pi}{4} \\ \sigma & \text{else} \end{cases}, \quad (7)$$

120 where  $\sigma \in [0, \sigma^{\max}]$ . For  $\sigma$ , 100 linearly spaced observation points between zero and  
 121 the maximum stress ( $\sigma^{\max} = 200$  kPa) are used. The resulting strains are calculated  
 122 by iteratively solving equation (5) for  $\lambda_{1,2}$  and thereby obtaining  $e_{1,2}$ . In practice, a  
 123 combination of angles can be successively tested. We refer to this combination as the  
 124 experimental protocol that needs to be optimally designed.

## 125 2.2. Information-theoretic framework for optimal design

126 The problem of optimal design typically refers to the choice of a design of ex-  
 127 periments such that the design is optimal with respect to a pre-determined statistical  
 128 criterion. We propose that the information-theoretic measures naturally define such  
 129 statistical criteria. The central idea is that information gain [21,22] from an experiment  
 130 or protocol—as quantified by the information-theoretic quantities of mutual information  
 131 and conditional mutual information—can be directly used as a reasonable statistical  
 132 criterion for optimal design. These quantities are described next after presenting the  
 133 framework for optimal design.

### 134 2.2.1. Optimal design problem

Consider the following general model:

$$\mathbf{y} = \mathcal{M}(\boldsymbol{\theta}), \quad (8)$$

135 where  $\mathcal{M}$  denotes for the forward model that takes  $\boldsymbol{\theta} \in \mathbb{R}^m$  and outputs  $\mathbf{y} \in \mathbb{R}^n$ . Note  
 136 that  $\boldsymbol{\theta}$  may contain initial and boundary conditions of the model and that  $\mathbf{y}$  may subsume

137 the output at many time-points in the case of a dynamical system. Subsequently, consider  
138 that the measurement model is as follows

$$\mathbf{z} = \mathcal{H}_p(\mathbf{y}, \boldsymbol{\theta}) + \boldsymbol{\varepsilon}, \quad (9)$$

139 where  $\mathcal{H}_p$  represents the observation operator,  $\mathbf{z} \in \mathbb{R}^d$  represents the measurement vector,  
140 and  $\boldsymbol{\varepsilon}$  represents the vector of measurement error/noise. Note that the the observation  
141 operator  $\mathcal{H}_p$  depends on the design of experiments, which specifies which quantities are  
142 measured. Given a set of possible  $\mathcal{H}_p = \{\mathcal{H}_1, \mathcal{H}_2, \dots, \mathcal{H}_h\}$ , and a statistical criterion  
143  $\mathcal{S}(\mathcal{H}_p)$  to be maximised, the optimal design is given by

$$\hat{\mathcal{H}}_p = \arg \max_{\mathcal{H}_p} \mathcal{S}(\mathcal{H}_p). \quad (10)$$

144 In the case of the biaxial experiments, the model  $\mathcal{M}$  represents the model for the  
145 force controlled experiment (sections 2.1.1 and 2.1.2) and  $\mathcal{H}_p$  essentially denotes the  
146 experimental protocol, see section 2.1.2, representing the combination of angles—each  
147 representing a straight line in the  $\sigma_{11}$ - $\sigma_{22}$  plane—along which the strain measurements  
148 of  $e_1$  and  $e_2$  are acquired. With the possible variation of each angle between 0 and  $\pi/2$ ,  
149 the set  $\Phi$  of possible angles  $\phi$  are constructed through a uniform discretisation of the  
150 space between 0 and  $\pi/2$  into  $\alpha$  levels, thus

$$\Phi = \{\phi_0, \phi_1, \dots, \phi_\alpha\}. \quad (11)$$

151 The possible set of protocols is then given by any combination of elements in  $\Phi$  with the  
152 restriction that the number of elements in a protocol be limited to  $\mathcal{C}$ . Thus, if  $\bar{\Phi} \subset \Phi$  is a  
153 subset of angles representing a protocol, our set of protocols is given by

$$\mathcal{H}_p = \{\bar{\Phi} \subset \Phi \mid 1 \leq |\bar{\Phi}| \leq \mathcal{C}\}, \quad (12)$$

154 where  $|\cdot|$  represents the number of elements in the set. In other words, we choose at  
155 least 1 and up to  $\mathcal{C}$  elements from  $\Phi$ , with the total elements in  $\mathcal{H}_p$  being

$$|\mathcal{H}_p| = \binom{\alpha}{1} + \binom{\alpha}{2} \dots + \binom{\alpha}{\mathcal{C}}. \quad (13)$$

### 156 2.2.2. Information-theoretic quantities for optimal design

157 In the framework of section 2.2.1, we propose that information-theoretic quantities  
158 of mutual information and conditional mutual information are a natural choice for the  
159 statistical criterion  $\mathcal{S}$ . Denoting the random variables associated with  $\boldsymbol{\theta}$  and  $\mathbf{z}$  as  $\Theta$   
160 and  $\mathbf{Z}$ , respectively, the mutual information (MI) between the parameters  $\Theta$  and the  
161 measurements  $\mathbf{Z}$  is defined as [21]

$$\mathcal{I}(\Theta; \mathbf{Z}) = \int_{\mathcal{X}_\Theta \times \mathcal{X}_Z} p_{\Theta, \mathbf{Z}}(\boldsymbol{\theta}, \mathbf{z}) \frac{p_{\Theta, \mathbf{Z}}(\boldsymbol{\theta}, \mathbf{z})}{p_\Theta(\boldsymbol{\theta})p_Z(\mathbf{z})} d\boldsymbol{\theta} d\mathbf{z}, \quad (14)$$

162 where  $p_X(x)$  represents the probability density of a random variable  $X$  with a realisation  
163  $X = x$  and support  $\mathcal{X}_X$ . The mutual information  $\mathcal{I}(\Theta; \mathbf{Z})$  quantifies the amount of  
164 information that can be gained on average by knowing one random variable, say  $\mathbf{Z}$ ,  
165 about the other, say  $\Theta$ . Indeed, with this interpretation, MI is a good candidate for the  
166 statistical criterion  $\mathcal{S}$  for optimal design. For an individual parameter,  $\Theta_i$ , or indeed  
167 for any combination of parameters  $\{\Theta_i, \Theta_j\}$ , the corresponding information gains can  
168 be similarly computed through  $\mathcal{I}(\Theta_i; \mathbf{Z})$  and  $\mathcal{I}(\{\Theta_i, \Theta_j\}; \mathbf{Z})$ , respectively. Thus, while  
169  $\mathcal{I}(\Theta_i; \mathbf{Z})$  quantifies the information gain individually for the parameter  $\Theta_i$ , the quantity  
170  $\mathcal{I}(\{\Theta_i, \Theta_j\}; \mathbf{Z})$  quantifies information gain for the pair  $\{\Theta_i, \Theta_j\}$  jointly. A measure of  
171 correlation between the parameters  $\Theta_i$  and  $\Theta_j$  is, however, missing, and is provided by  
172 conditional mutual information (CMI) defined as

$$\underbrace{\mathcal{I}(\Theta_i; \Theta_j | \mathbf{Z})}_I = \underbrace{\mathcal{I}(\Theta_i; \{\Theta_j, \mathbf{Z}\})}_{II} - \underbrace{\mathcal{I}(\Theta_i; \mathbf{Z})}_{III}. \quad (15)$$

173 The CMI  $\mathcal{I}(\Theta_i; \Theta_j | \mathbf{Z})$  represents the additional information gained about the pa-  
 174 rameter  $\Theta_i$  when both  $\Theta_j$  and  $\mathbf{Z}$  are known (term II) relative to when only the measure-  
 175 ments  $\Theta_i$  alone are known (term III). Note that CMI is symmetric, i.e.  $\mathcal{I}(\Theta_i; \Theta_j | \mathbf{Z}) =$   
 176  $\mathcal{I}(\Theta_j; \Theta_i | \mathbf{Z})$ , and can be interpreted as a measure of dependence between the parameters  
 177 given the measurements  $\mathbf{Z}$ . Also note that both MI and CMI are non-negative.

178 With the above background, many statistical measures can be constructed. For  
 179 example:

- 180 1. The mutual information for any single parameter may be maximised, giving  $\mathcal{S} =$   
 181  $\mathcal{I}(\Theta_i; \mathbf{Z})$ . This approach only concerns with the posterior of the parameter  $\Theta_i$  and  
 182 ignores all other parameters.
- 183 2. The joint mutual information may be maximised, giving  $\mathcal{S} = \mathcal{I}(\Theta; \mathbf{Z})$ . In the sense  
 184 of classical optimal design this can be interpreted as the D-optimal design. This is  
 185 because D-optimal designs minimise the determinant of the Fisher Information  
 186 Matrix inverse, and  $\mathcal{S} = \mathcal{I}(\Theta; \mathbf{Z})$  measures the information gain in the joint  $\Theta$   
 187 space.
- 188 3. The sum of individual parameter mutual information may be be maximised, giving  
 189  $\mathcal{S} = \sum_{i=1}^m \mathcal{I}(\Theta_i; \mathbf{Z})$ . In the sense of classical optimal design this can be interpreted  
 190 as the A-optimal design. This is because the the A-optimal design minimises the  
 191 trace of the Fisher Information Matrix inverse, and  $\mathcal{S} = \sum_{i=1}^m \mathcal{I}(\Theta_i; \mathbf{Z})$  measures  
 192 the sum of the information gains for all the parameters.
- 193 4. Alternatively, one may seek to maximise individual parameter information gain  
 194 while minimising pairwise CMI, thus seeking both small posterior variances and  
 195 minimising pairwise correlations between the parameters. In this case, the statistical  
 196 criterion is

$$\mathcal{S} = \sum_{i=1}^m \mathcal{I}(\Theta_i; \mathbf{Z}) - \tau \sum_{i=1}^m \sum_{j=i}^m \mathcal{I}(\Theta_i; \Theta_j | \mathbf{Z}), \quad (16)$$

197 where  $\tau > 0$  is a regularisation parameter.

198 Note that the above list is not exhaustive, and based on the interpretations of MI  
 199 and CMI, other criteria may be constructed based on the desired sense of optimality.

### 200 2.2.3. Estimating mutual information

201 In general, the forward model in equation (8) is non-linear, and hence even if the  
 202 observation operator is linear (implying linear combinations of the state are measured),  
 203 the analytical computation of mutual information is intractable. Thus, the information-  
 204 theoretic quantities of MI and CMI must be estimated. A common method is to generate  
 205 samples of  $\Theta$  through specification of an appropriate prior probability density  $p_{\Theta}(\theta)$ .  
 206 Denoting these  $N_s$  samples as  $\theta^{(i)}, i = \{1, 2, \dots, N_s\}$ , each  $\theta^{(i)}$  can be propagated through  
 207 the forward and observation models of equations (8) and (9) to produce corresponding  
 208 samples of  $\mathbf{Z}$ , denoted as  $\mathbf{z}^{(i)}$ . The samples of  $\theta^{(i)}$  and  $\mathbf{z}^{(i)}$  can subsequently be used on  
 209 non-parametric estimators of MI and CMI. Such non-parametric estimators can broadly  
 210 be classified into two categories: kernel density estimators (KDE) [23] and  $k$ -nearest  
 211 neighbour (kNN) estimators [24,25]. For an overview of such methods, we refer to [26].  
 212 While the estimator proposed by Kraskov et. al. [24] is widely used and performs very  
 213 well across a range of scenarios, one of its drawbacks is that it suffers from higher errors  
 214 when extreme correlations are present between the variables and/or when the the data  
 215 effectively lives in a lower-dimensional manifold. Since we are working with models that  
 216 specify explicit relationships between the variables through the forward and observation  
 217 model, this is likely to be true for the data-set of  $(\theta^{(i)}, \mathbf{z}^{(i)})$ . Thus, in this study, we

218 employ the local non-uniformity correction (LNC) proposed in [27], which includes a  
 219 correction term to the original estimator by Kraskov et. al. [24]. This term accounts for  
 220 strong dependencies between the variables through local principle component analysis  
 221 [27]. The method of [27] is used for estimation of all MIs, and CMI's are estimated from  
 222 the difference of two MIs, see equation (15).

#### 223 2.2.4. Dimensionality reduction for the biaxial experiment

224 One of the main difficulties in estimating information theoretic quantities is re-  
 225 lated to the data dimension. The non-parametric estimation is particularly challenging  
 226 whenever the data are close to manifolds embedded in high-dimensional spaces. This is  
 227 indeed the case when a physical model relates parameters and observable quantities.  
 228 One of the possible ways to overcome this difficulty or, at least, to mitigate it, is (dimen-  
 229 sion or) model reduction, which aims at discovering the underlying low-dimensional  
 230 structure of a set of data (a comprehensive review of the topic can be found in [28–31]).  
 231 A large spectrum of methods have been proposed in the literature. In the present con-  
 232 tribution, we adopt a local reduced-basis method (similar, in the spirit, to the methods  
 233 proposed in [32,33]). Let the strains computed by the model be  $e_{1,2}(\sigma; \phi; k_1, k_2)$ , where  
 234  $k_1$  and  $k_2$  are the model parameters  $(k_1, k_2) \in \Omega_k \subset \mathbb{R}^2$ , and  $\sigma \in \Omega_\sigma \subset \mathbb{R}$  is the variable  
 235 defined in section 2.1.2. Let  $n \in \mathbb{N}^*$ , we introduce the following approximation:

$$e_{1,2} \approx \sum_{i=1}^n \eta_i r_i(\sigma, \phi) s_i(k_1, k_2, \phi), \quad (17)$$

236 which is well defined by virtue of the Eckart-Young theorem. First, let us observe that  
 237 a given protocol consists in a set of known angles  $\bar{\Phi}$ . An efficient way to construct the  
 238 local reduced basis is hence to introduce a Proper Orthogonal Decomposition (POD) for  
 239 each of the angles  $\phi_j \in \bar{\Phi}$ . This corresponds to looking for an approximation of the form:

$$e_{1,2}^{(j)}(\sigma; \phi_j; k_1, k_2) \approx \sum_{i=1}^n \eta_i^{(j)} r_i^{(j)}(\sigma) s_i^{(j)}(k_1, k_2), \quad (18)$$

240 where  $\langle r_i^{(j)}, r_k^{(j)} \rangle_{\Omega_\sigma} = \delta_{ik}$  and  $\langle s_i^{(j)}, s_k^{(j)} \rangle_{\Omega_k} = \delta_{ik}$  ( $\langle \cdot, \cdot \rangle_{\Omega_\sigma, \Omega_k}$  being the standard  $L^2$  scalar  
 241 product). The error in the approximation is related to the number  $n$  of modes retained:

$$\|e_{1,2}^{(j)} - \sum_{i=1}^n \eta_i^{(j)} r_i^{(j)}(\sigma) s_i^{(j)}(k_1, k_2)\|_{L^2(\Omega_\sigma \times \Omega_k)}^2 = \sum_{i=n+1}^{\infty} \eta_i^{(j)2} \quad (19)$$

In the present work, a number  $n = 4$  modes proved to be sufficient in order to get  
 errors smaller than  $10^{-3}$  in  $L^2$  norm on the solution reconstruction. This means that  
 the set of elements  $e_{1,2}(\sigma; \phi_j; k_1, k_2)$  are close to the linear subspace spanned by the first  
 $n = 4$  modes  $r_i^{(j)}$ . Henceforth, instead of considering the discretised  $e_{1,2}$  we will consider  
 their coordinates in the subspace, given by:

$$z_{1,2}^{(j)}|_i = \langle e_{1,2}, r_i^{(j)} \rangle_{\Omega_\sigma} = \eta_i^{(j)} s_i^{(j)}(k_1, k_2). \quad (20)$$

#### 242 2.2.5. Validation of results against existing methods

243 Several methods and criteria to define and reach an optimal design of experiments  
 244 were proposed [12]. Among them, D-optimality criterion attempts at maximising  
 245 the determinant of the information matrix. In the present case, this is equivalent to  
 246 minimize the determinant of the inverse of the average Hessian of the loss function we  
 247 would introduce in a classical parameter estimation method. In a noisy setting, and,  
 248 in particular, when the noise is Gaussian, this cost function is equivalent to minus the  
 249 logarithm of the likelihood function. Let the misfit function be  $f(\theta)$  and  $\mathbb{E}_\Theta$  denote the  
 250 expectation operator. The average of the Hessian reads:

$$H = \mathbb{E}_{\Theta}[\partial_{\theta}^2 f|_{\theta_*}], \quad (21)$$

251 where  $\theta_*$  is the value of the parameter minimising the loss function.

### 252 2.2.6. Overview of approach for the biaxial experiments

253 In the context of the biaxial experiments, the parameters are  $k_1$  and  $k_2$ , represented  
 254 as random variables  $K_1$  and  $K_2$ , respectively. The variability in these parameters is  
 255 considered to be uniform (thus imposing a uniform prior distribution) in the following  
 256 intervals:  $k_1 \in [5, 100]$  kPa and  $k_2 \in [5, 80]$ . For a single value of angle  $\phi$ , the measure-  
 257 ments are the strain values  $e_1$  and  $e_2$  and measured at 100 points along the line defined  
 258 by the angle  $\phi$ . Here, we consider  $\alpha = 16$  discrete values of possible measurement angles  
 259  $\phi$  uniformly distributed between, and including,  $0^\circ$  and  $90^\circ$ . For each angle  $\phi$ , separate  
 260 reduced bases of 4 modes for  $e_1$  and  $e_2$  are constructed through POD over 400 values  
 261 of  $(K_1, K_2)$  sampled uniformly in the aforementioned parametric space. Thus, for any  
 262 angle  $\phi$ , the dimensionality reduction approach projects  $e_1$  and  $e_2$  measured at 100 points  
 263 along the line defined by  $\phi$  to a basis of 4+4 modes. For a given protocol consisting of  
 264 multiple angles, the measurement vector  $\mathbf{z}$  (with corresponding random variable  $\mathbf{Z}$ ), is  
 265 the collection of all the reduced basis representation of  $e_1$  and  $e_2$  along the angles in the  
 266 protocol. Lastly, the maximum number of angles in a protocol is restricted to  $\mathcal{C} = 5$ ,  
 267 giving a total of 6,884 unique combinations of the  $\alpha = 16$  angles.

268 For the estimation of MI and CMI, a total of  $N = 10,000$  values of  $(K_1, K_2)$  are  
 269 uniformly distributed in the parametric space. For each such sample  $(k_1^{(i)}, k_2^{(i)})$ , the  
 270 numerical model of the biaxial experiment is run to produce  $e_1^{(i)}$  and  $e_2^{(i)}$ , which are  
 271 then projected on to the reduced basis, giving  $\mathbf{z}^{(i)}$ . The  $N$  triplets of  $(k_1^{(i)}, k_2^{(i)}, \mathbf{z}^{(i)})$  are  
 272 subsequently used for estimation of MI and CMI through the LNC estimator (see section  
 273 2.2.3). In equation (16) we use  $\tau = 1$ .

## 274 3. Results and discussion

275 For all the 6,884 combinations of angles, three statistical criteria are evaluated: (i)  
 276  $\mathcal{I}(A; \mathbf{Z})$ ; (ii)  $\mathcal{I}(B; \mathbf{Z})$ ; and (iii)  $\mathcal{I}(K_1; \mathbf{Z}) + \mathcal{I}(K_2; \mathbf{Z}) - \mathcal{I}(K_1; K_2 | \mathbf{Z})$ . While the first two  
 277 criteria aim to maximise information gain about  $A$  and  $B$  individually, the third criterion  
 278 aims to maximise information gain about  $A$  and  $B$  simultaneously while minimising  
 279 the information dependence between them. Figures 2–4 show the variation in these  
 280 three criterion when grouped by the number of angles in a protocol. In these Figures the  
 281 values of information criterion when using two approaches to uniformly discretise the  
 282 angular space within protocols is also presented. Observations from these plots are as  
 283 follows:

- 284 1. Generally, all the three information criteria increase with increasing number of  
 285 angles in the protocol. Intuitively, this is expected as higher number of angles imply  
 286 more measurement data and hence a higher potential for improved estimation  
 287 of the parameters. This observation is true for the maximum information gain,  
 288 minimum information gain, and the mean information gain.
- 289 2. Across all the three criteria, it is observed that the uniform discretisation is not  
 290 necessarily reflective of the best protocol for estimating the parameters. In fact,  
 291 in most cases, the performance of uniform discretisation is close to the mean  
 292 information gain observed across all the angle combinations.
- 293 3. From Figures 2 and 3 it is observed that the angular combinations that maximise  
 294 information gain for  $K_1$  are not identical—and vary significantly when more than 2  
 295 angles are simultaneously used—to those that maximise information gain for  $K_2$ .  
 296 This further motivates the use of a criterion that balances information gains in both  
 297 the parameters while minimising their interdependence.
- 298 4. Figure 4 shows that the best combinations that maximises a balanced criterion such  
 299 as  $\mathcal{I}(K_1; \mathbf{Z}) + \mathcal{I}(K_2; \mathbf{Z}) - \mathcal{I}(K_1; K_2 | \mathbf{Z})$  are a trade-off between the combinations of

- 300 angles that maximises  $\mathcal{I}(K_1; \mathbf{Z})$  and  $\mathcal{I}(K_2; \mathbf{Z})$  individually. For example, when 5  
 301 angles are considered, the angles that maximise  $\mathcal{I}(K_1; \mathbf{Z})$  are  $\phi_a = [66, 72, 78, 84, 90]$ ,  
 302 those that maximise  $\mathcal{I}(K_2; \mathbf{Z})$  are  $\phi_b = [30, 36, 42, 48, 54]$ , while the combination that  
 303 maximises  $\mathcal{I}(K_1; \mathbf{Z}) + \mathcal{I}(K_2; \mathbf{Z}) - \mathcal{I}(K_1; K_2 | \mathbf{Z})$  is  $[30, 36, 48, 78, 90]$ , which has two  
 304 angles from  $\phi_a$  and three angles from  $\phi_b$ . It should be noted that such a trade-off  
 305 between maximising individual parameter gains is still significantly different than  
 306 a uniform discretisation.
- 307 5. Finally, it is observed that the worst combinations are all low angles:  $[0, 6, 12, 18, 24]$ .  
 308 This can be related to the fact that at low angles, the applied stress is largely aligned  
 309 along the stiff fibers of the tissue, thus resulting in lower strain values. Thus, the  
 310 lower angles provide a small range of the observations, while the larger angles  
 311 provide a larger range (Fig. 9a), thereby containing more information about the  
 312 parameters.

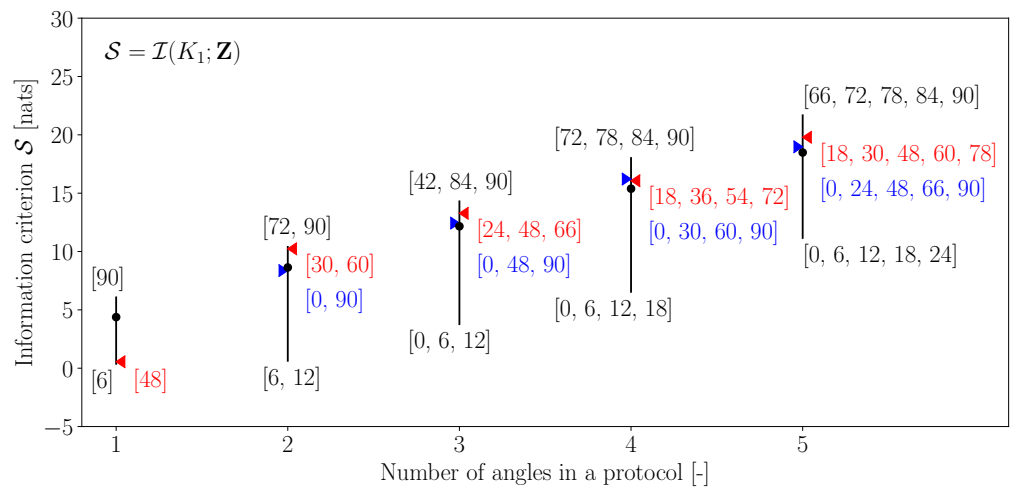


**Figure 2.** The variation of information criterion  $\mathcal{S} = \mathcal{I}(K_1; \mathbf{Z})$  across the 6,884 combinations grouped by the number of angles in a protocol. The vertical lines represent the variation around the mean value, which is shown in black circles. Black text shows the combinations that produce maximum and minimum values of  $\mathcal{S}$ . The red and blue pointers show  $\mathcal{S}$  for angle combinations that follow a uniform discretisation of the angular space between 0 and 90 degrees. Red and blue texts show the associated angle combinations.

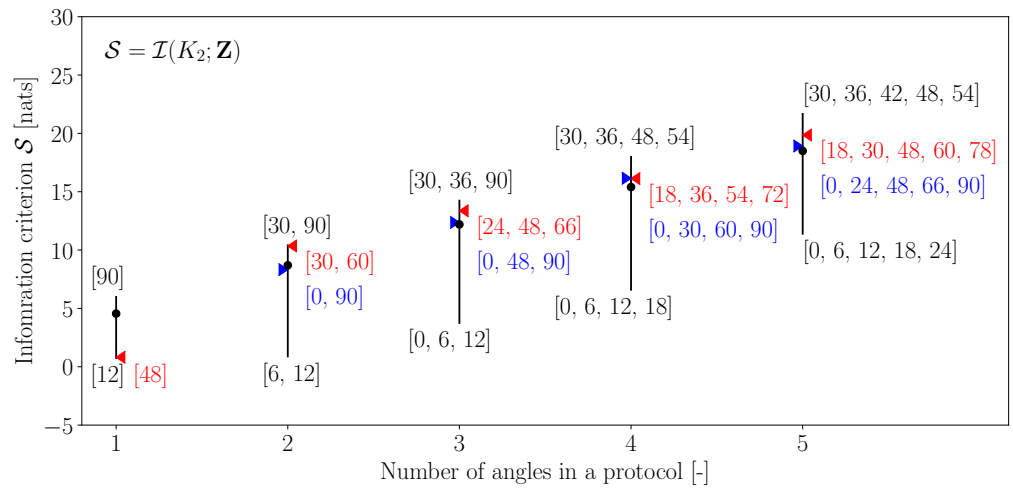


**Figure 3.** The variation of information criterion  $S = \mathcal{I}(K_2; \mathbf{Z})$  across the 6,884 combinations grouped by the number of angles in a protocol. The vertical lines represent the variation around the mean value, which is shown in black circles. Black text shows the combinations that produce maximum and minimum values of  $S$ . The red and blue pointers show  $S$  for angle combinations that follow a uniform discretisation of the angular space between 0 and 90 degrees. Red and blue texts show the associated angle combinations.

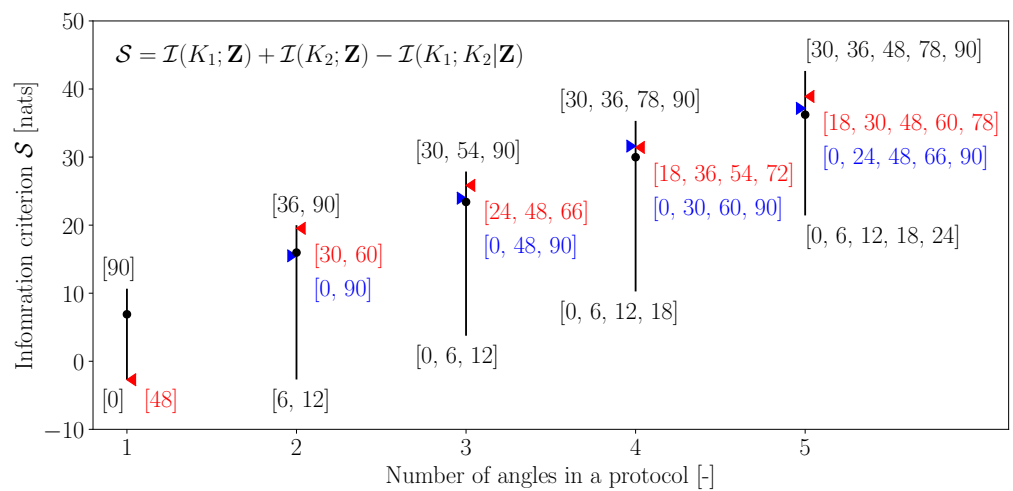


**Figure 4.** The variation of information criterion  $S = \mathcal{I}(K_1; \mathbf{Z}) + \mathcal{I}(K_2; \mathbf{Z}) - \mathcal{I}(K_1; K_2 | \mathbf{Z})$  across the 6,884 combinations grouped by the number of angles in a protocol. The vertical lines represent the variation around the mean value, which is shown in black circles. Black text shows the combinations that produce maximum and minimum values of  $S$ . The red and blue pointers show  $S$  for angle combinations that follow a uniform discretisation of the angular space between 0 and 90 degrees. Red and blue texts show the associated angle combinations.

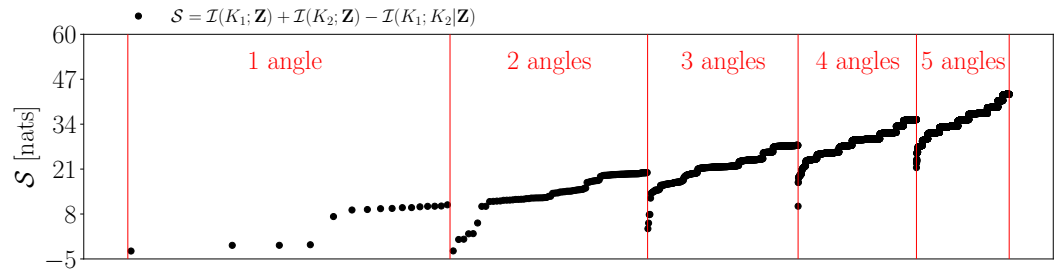


**Figure 5.** The variation of information criterion  $\mathcal{S} = \mathcal{I}(K_1; \mathbf{Z}) + \mathcal{I}(K_2; \mathbf{Z}) - \mathcal{I}(K_1; K_2 | \mathbf{Z})$  across the 6,884 combinations. The vertical red lines show the groupings with respect to the number of angles in a protocol and  $\mathcal{S}$  values are sorted in increasing order within each such grouping. The x-axis is represents the index associated with the protocol and is in logarithmic scale to capture the spread between 1 angle in a protocol (16 values) vs 5 angles in a protocol (4,368 values).

313 From this point onward, we present results only for the balanced information  
 314 criterion  $\mathcal{S} = \mathcal{I}(K_1; \mathbf{Z}) + \mathcal{I}(K_2; \mathbf{Z}) - \mathcal{I}(K_1; K_2 | \mathbf{Z})$ . Figure 5 shows the variation in  $\mathcal{S}$   
 315 across all the combinations (x-axis, and in log-scale to capture the spread) grouped  
 316 by the number of angles in a protocol and sorted in increasing order of  $\mathcal{S}$  within  
 317 each group. Within each group, when observing the minimum and maximum values  
 318 of  $\mathcal{S}$ , it shows that a better choice of angles can lead to more than 100% increase in  
 319 the information gain compared to a poor choice. Furthermore, it shows that good  
 320 combinations of a lower number of angles can lead to higher information gain compared  
 321 to higher number of angles with bad combinations. For example, the maximum  $\mathcal{S}$   
 322 when only one angle is used is higher than many combinations with 2–4 angles. This  
 323 emphasises the utility of optimal design and the proposed framework.

324 Figure 6 shows  $\mathcal{S}$  for all the 6,884 combinations in increasing order of magnitude and  
 325 Figure 7 shows a zoomed plot for the first 150 combinations along with the corresponding  
 326 combinations of angles. Observing index values of 26 (red) and 28 (blue) in Figure 7  
 327 shows that even though four combinations are used in index 26 protocol, it produces a  
 328 lower  $\mathcal{S}$  compared to only a single angle used in index 28 protocol. Furthermore, since  
 329 Figure 7 shows the first 150 out of 6,884 combinations of Figure 6 (which is sorted in  
 330 creasing order of  $\mathcal{S}$ ), all combinations here are relatively low  $\mathcal{S}$  producing protocols.  
 331 Observing the high density of angles in the region  $\phi < 24^\circ$ , is indicative that lower  
 332 values of angles, in particular those less than  $24^\circ$  are relatively less informative when  
 333 compared to higher values of angles. This behaviour is also apparent in Figure 8, which  
 334 shows  $\mathcal{S}$  values for protocols that use only one angle, and where a sharp jump can be  
 335 observed when transitioning from  $18^\circ$  to  $24^\circ$ . This peculiar behaviour may be explained  
 336 by the physics of the biaxial experiment. Looking at the resulting strains  $e_1$  and  $e_2$  at this  
 337 transition (Fig. 9b), we observe that the  $e_1$  changes from positive to negative values. This  
 338 behavior captures the important coupling between the two normal stresses and strains  
 339 and is also related to the fiber dispersion in our constitutive model (equation (1), [18]). It  
 340 is remarkable and encouraging that the information-theoretic framework captures the  
 341 physics of the problem without explicitly considering it in the framework. While for  
 342 simpler low-dimensional models the association between physics and optimal design  
 343 may be relatively easy to see, inferring such behaviour is, in general, not trivial for more  
 344 complex and higher-dimensional models.

345 Similarly to Figure 8, the results of the information-theoretic optimal design and  
 346 further be analysed for higher number of angles. When two angles are considered, the  $\mathcal{S}$   
 347 values in increasing order of magnitude and the corresponding angle combinations, are  
 348 shown in Figure 10. This figure re-iterates observations made previously: i) the choice  
 349 of combinations significantly affects the information gain, the best combination gives

350 approximately 20 nats more information compared to the worst combination; and ii)  
 351 generally speaking, higher angles are more informative compared to lower angles, in  
 352 particular angles below  $24^\circ$ . While similar analysis for more than two angle combinations  
 353 can be easily performed, efficient visual representation of such results is cumbersome  
 354 and avoided in this manuscript.

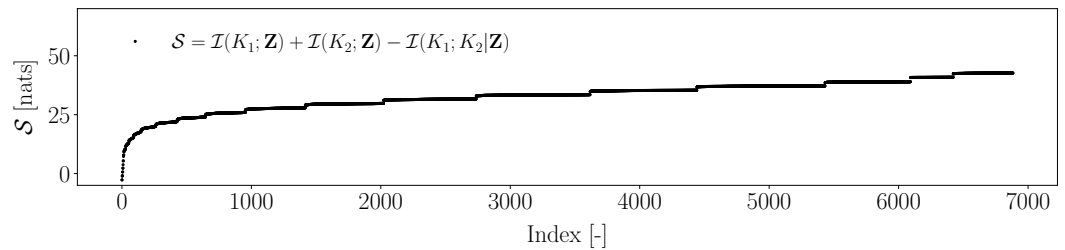


**Figure 6.** The variation of information criterion  $\mathcal{S} = \mathcal{I}(K_1; \mathbf{Z}) + \mathcal{I}(K_2; \mathbf{Z}) - \mathcal{I}(K_1; K_2 | \mathbf{Z})$  across the 6,884 combinations sorted in increasing order of  $\mathcal{S}$

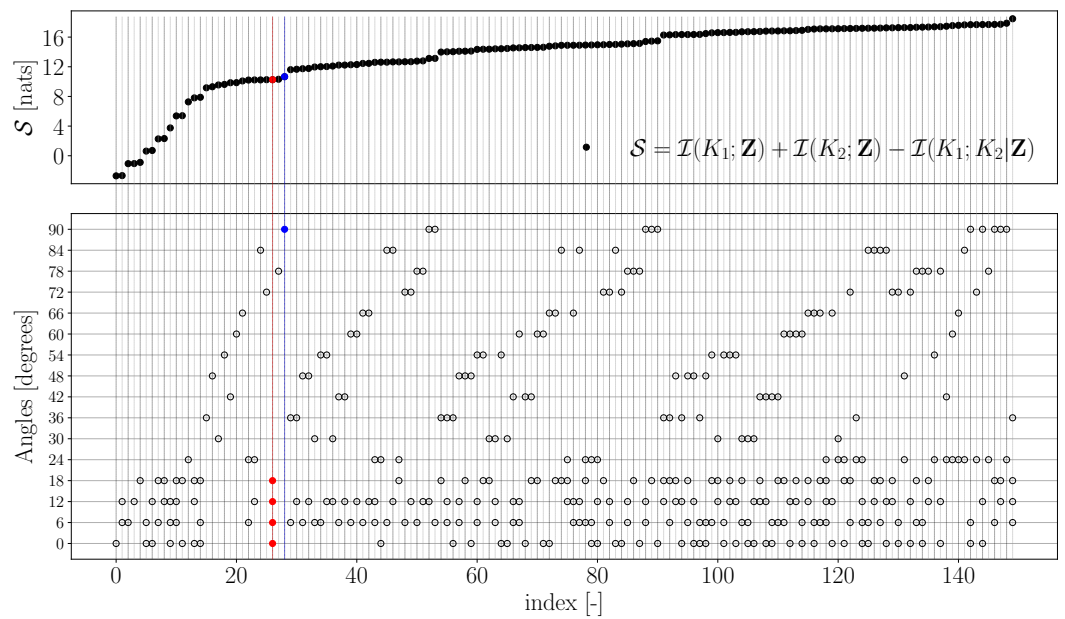


**Figure 7.** Zoomed view into the first 150 protocols from Figure 6. The upper panel shows  $\mathcal{S}$  and the lower panel shows the angles (by circles) in the corresponding protocol.

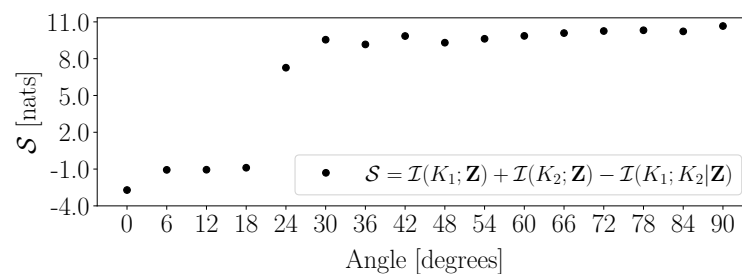


**Figure 8.** Information criterion against the angle when the protocols are restricted to a maximum of one angle.

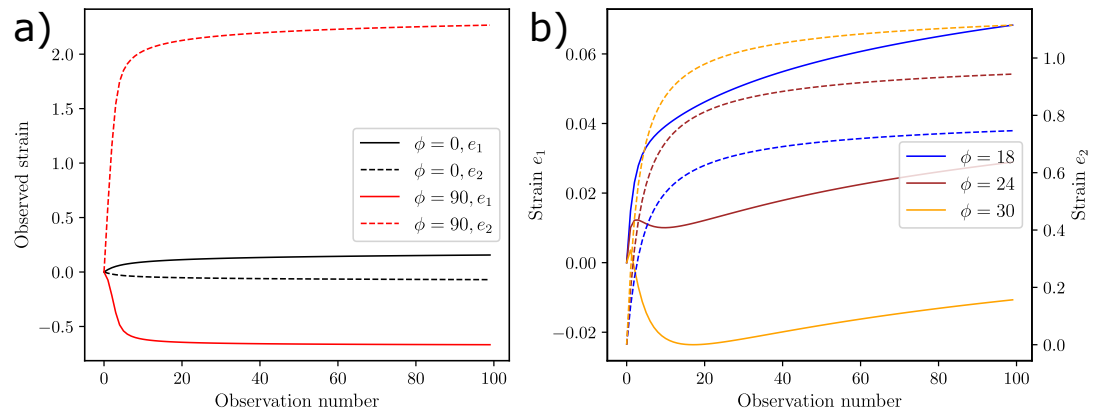


**Figure 9.** Representative observations from the model with  $k_1 = 40$  kPa and  $k_2 = 40$ . a) The observations using angles  $\phi = 0$  and  $90$  degrees, with the latter covering a significantly larger range. b) The change in observations the angle is changed from  $18$ ,  $24$ , to  $30$  degrees shows a transition in  $e_1$  from positive to negative values, indicating a coupling between the two directions.

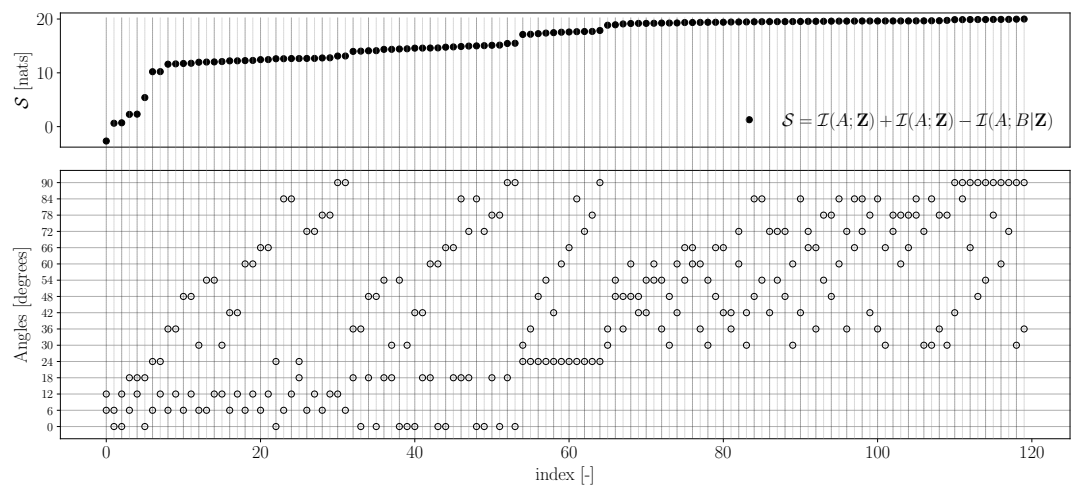


**Figure 10.** Information criterion against the angles when the protocols are restricted to only two angles. The upper panel shows  $S$  and the lower panel shows the angles (by circles) in the corresponding protocol.

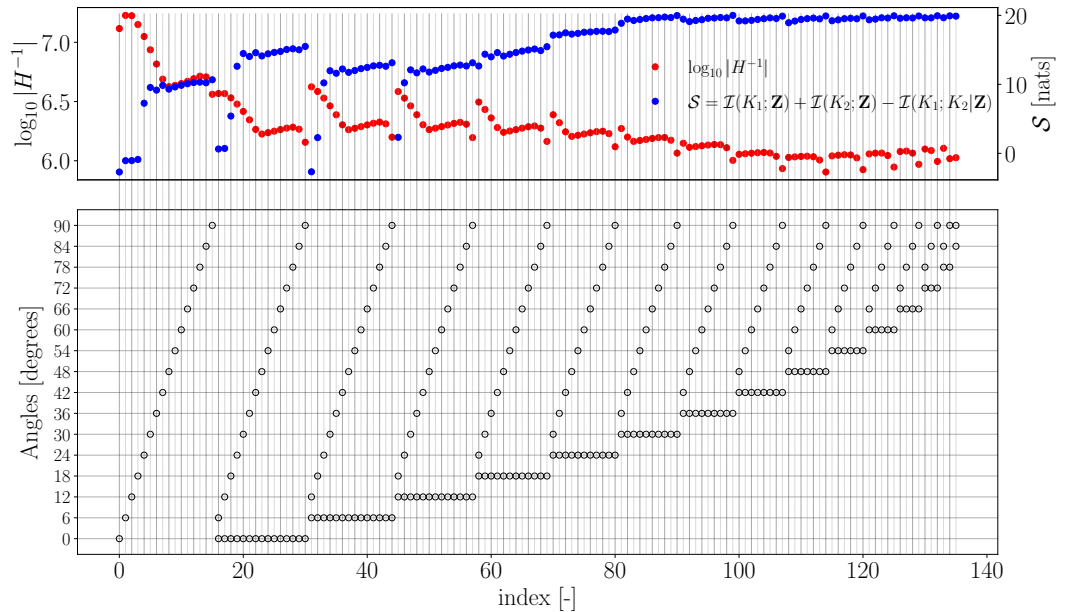


**Figure 11.** Information criterion  $S$  (in blue) and the log of the determinant of the Fisher Information Matrix inverse  $\log_{10} |H^{-1}|$  (in red) against the angles when the protocols are restricted to a maximum of two angles. The upper panel shows  $S$  and  $\log_{10} |H^{-1}|$ , while the lower panel shows the angles (by circles) in the corresponding protocol. Note that here  $e_1$  is shown in solid lines (left y-axis) and  $e_2$  is shown in dashed lines (right y-axis).

355 To further illustrate the validity of the information-theoretic approach, comparison  
 356 with a classical method, see section 2.2.5, is presented. For one and two angles in a  
 357 protocol, Figure 11 shows a comparison between  $S$  and the log of the determinant of  
 358 the Fisher Information Matrix inverse,  $\log |H^{-1}|$ . It is encouraging that a high corre-  
 359 spondence between the two metrics is observed. In particular, increases in  $S$ , implying  
 360 higher information gains, are accompanied by corresponding decreases in  $\log |H^{-1}|$ ,  
 361 implying a smaller volume of the parameter posteriors. A Pearson correlation coefficient  
 362 of  $r = -0.76$  is observed between  $S$  and  $\log |H^{-1}|$  implying a high similarity between the  
 363 two metrics, and validating the information-theoretic approach in part. Let us remark  
 364 that, when the number of the parameters become large, evaluating the Hessian would  
 365 imply a non-negligible computational cost. On the contrary, the method used to evaluate  
 366 the Mutual Information, being a primarily Monte Carlo based estimation, is less severely  
 367 dependent on the number of parameters. Furthermore, computation of derivatives  
 368 (either numerically or through adjoint based methods) may be cumbersome for certain  
 369 type of models. Finally, we note that the effect of noise on information gain, and hence  
 370 optimal design, can be easily assessed in the proposed framework by adding noise to  
 371 the samples of  $\mathbf{Z}$ , see equation (9).

#### 372 4. Conclusion

373 A framework for optimal design based on information-theoretic quantities of mutual  
 374 information and conditional mutual information is proposed. The framework treats  
 375 information gain as the central criterion for inverse problems and proposes several  
 376 information-theoretic frameworks for desired sense of optimality. The capabilities of  
 377 this framework are tested on the optimal design problem for biaxial experiments, where  
 378 the effect of angle combinations along which the strains are measured is assessed on  
 379 parameter estimation through information gain. Without including any physics based  
 380 reasoning and purely through the information-theoretic measures, it is found that low  
 381 angles  $\leq 24^\circ$  are not very informative about the parameters relative to high angles.

382 These observations are then found to be consistent based on physics-based reasoning,  
383 thereby showing the efficacy of the proposed framework. Furthermore, it is demon-  
384 strated measurements for a low total number of angles which are carefully chosen can  
385 be more informative compared to the case when measurements along a high number  
386 of poorly chosen angles are acquired, thus highlighting both the importance of optimal  
387 design for biaxial experiments and the utility of the proposed framework in uncovering  
388 good angle combinations. Relation of the proposed framework to classical optimal  
389 design is performed and shown that the results produced by the new framework are  
390 consistent with classical frameworks.

## 391 5. Limitations and future work

392 While the proposed framework is shown to perform well on a two-parameter  
393 problem, its performance in higher parameter problems is not assessed. This assessment  
394 forms the the primary limitation and area of future assessment. In particular, the  
395 problems envisaged are largely related to the performance of the MI and CMI estimators  
396 in higher dimensions of both parameters and the measurements. While a dimensionality  
397 reduction approach was adopted in this study to minimise the adverse effects of the  
398 latter, this may not be possible in many forward and inverse problems. Thus, a large area  
399 of future work relates to the development of efficient and robust MI and CMI estimators.  
400 Lastly, a thorough comparison against classical optimal design methods (C-, E-, T-,  
401 V-optimal designs, etc.) needs to be performed, along with the construction and analysis  
402 of corresponding information-theoretic metrics.

403 **Author Contributions:** All authors contributed equally to writing, editing, and reviewing the  
404 manuscript. SP and DL conceptualised the information-theoretic framework. AA and SP con-  
405 ceptualised the application to the biaxial experiments. AA wrote the numerical code for the  
406 biaxial experiment. SP and DL wrote the code for dimensionality reduction and estimation of  
407 information-theoretic measures. All authors contributed equally to the analysis of the results.

408 **Funding:** This research was funded by the Engineering and Physical Sciences Research Coun-  
409 cil of the UK (Grant reference EP/R010811/1 to SP) and (Grant reference EP/P018912/1 and  
410 EP/P018912/2 to AA).

411 **Conflicts of Interest:** The authors declare no conflict of interest.

## References

1. Holzapfel, G.A. *Nonlinear solid mechanics*; Vol. 24, Wiley Chichester, 2000.
2. Zhang, W.; Feng, Y.; Lee, C.H.; Billiar, K.L.; Sacks, M.S. A generalized method for the analysis of planar biaxial mechanical data using tethered testing configurations. *Journal of biomechanical engineering* **2015**, *137*, 064501.
3. Labrosse, M.R.; Jafar, R.; Ngu, J.; Boodhwani, M. Planar biaxial testing of heart valve cusp replacement biomaterials: Experiments, theory and material constants. *Acta Biomaterialia* **2016**, *45*, 303–320.
4. Humphrey, J.; Yin, F. On constitutive relations and finite deformations of passive cardiac tissue: I. A pseudostrain-energy function. *Journal of biomechanical engineering* **1987**, *109*, 298–304.
5. Laurence, D.; Ross, C.; Jett, S.; Johns, C.; Echols, A.; Baumwart, R.; Towner, R.; Liao, J.; Bajona, P.; Wu, Y.; Lee, C.H. An investigation of regional variations in the biaxial mechanical properties and stress relaxation behaviors of porcine atrioventricular heart valve leaflets. *Journal of Biomechanics* **2019**, *83*, 16–27. doi:<https://doi.org/10.1016/j.jbiomech.2018.11.015>.
6. Jett, S.V.; Hudson, L.T.; Baumwart, R.; Bohnstedt, B.N.; Mir, A.; Burkhart, H.M.; Holzapfel, G.A.; Wu, Y.; Lee, C.H. Integration of polarized spatial frequency domain imaging (pSFDI) with a biaxial mechanical testing system for quantification of load-dependent collagen architecture in soft collagenous tissues. *Acta Biomaterialia* **2020**, *102*, 149–168. doi:<https://doi.org/10.1016/j.actbio.2019.11.028>.
7. Billiar, K.L.; Sacks, M.S. Biaxial mechanical properties of the native and glutaraldehyde-treated aortic valve cusp: part II—a structural constitutive model. *Journal of biomechanical engineering* **2000**, *122*, 327–335.
8. Ross, C.; Laurence, D.; Wu, Y.; Lee, C.H. Biaxial Mechanical Characterizations of Atrioventricular Heart Valves. *Journal of visualized experiments : JoVE* **2019**. doi:10.3791/59170.
9. Maurel, W.; Thalmann, D.; Wu, Y.; Thalmann, N.M., Constitutive Modeling. In *Biomechanical Models for Soft Tissue Simulation*; Springer Berlin Heidelberg: Berlin, Heidelberg, 1998; pp. 79–120.
10. Holzapfel, G.A.; Gasser, T.C.; Ogden, R.W. A new constitutive framework for arterial wall mechanics and a comparative study of material models. *Journal of elasticity and the physical science of solids* **2000**, *61*, 1–48.

11. May-Newman, K.; Yin, F.C.P. A constitutive law for mitral valve tissue. *Journal of Biomechanical Engineering* **1998**, *120*, 38–47. doi:10.1115/1.2834305.
12. Pukelsheim, F. *Optimal design of experiments*; SIAM, 2006.
13. Banks, H.T.; Holm, K.; Kappel, F. Comparison of optimal design methods in inverse problems. *Inverse problems* **2011**, *27*, 075002.
14. Banks, H.T.; Dediu, S.; Ernstberger, S.L.; Kappel, F. Generalized sensitivities and optimal experimental design **2010**.
15. Banks, H.T.; Rubio, D.; Saintier, N.; Troparevsky, M.I. Optimal design techniques for distributed parameter systems. 2013 Proceedings of the Conference on Control and its Applications. SIAM, 2013, pp. 83–90.
16. Sebastiani, P.; Wynn, H.P. Maximum entropy sampling and optimal Bayesian experimental design. *Journal of the Royal Statistical Society: Series B (Statistical Methodology)* **2000**, *62*, 145–157.
17. Capellari, G.; Chatzi, E.; Mariani, S.; others. Parameter identifiability through information theory. Proceedings of the 2nd ECCOMAS Thematic Conference on Uncertainty Quantification in Computational Sciences and Engineering (UNCECOMP), Rhodes Island, Greece, 2017, pp. 15–17.
18. Gasser, T.C.; Ogden, R.W.; Holzapfel, G.A. Hyperelastic modelling of arterial layers with distributed collagen fibre orientations. *Journal of The Royal Society Interface* **2006**, *3*, 15–35. doi:10.1098/rsif.2005.0073.
19. Aggarwal, A. An improved parameter estimation and comparison for soft tissue constitutive models containing an exponential function. *Biomechanics and Modeling in Mechanobiology* **2017**, *16*, 1309–1327. doi:10.1007/s10237-017-0889-3.
20. Aggarwal, A. Effect of Residual and Transformation Choice on Computational Aspects of Biomechanical Parameter Estimation of Soft Tissues. *Bioengineering* **2019**, *6*. doi:10.3390/bioengineering6040100.
21. Pant, S.; Lombardi, D. An information-theoretic approach to assess practical identifiability of parametric dynamical systems. *Mathematical biosciences* **2015**, *268*, 66–79.
22. Pant, S. Information sensitivity functions to assess parameter information gain and identifiability of dynamical systems. *Journal of The Royal Society Interface* **2018**, *15*, 20170871.
23. Moon, Y.I.; Rajagopalan, B.; Lall, U. Estimation of mutual information using kernel density estimators. *Physical Review E* **1995**, *52*, 2318.
24. Kraskov, A.; Stögbauer, H.; Grassberger, P. Estimating mutual information. *Physical Review E* **2004**, *69*, 066138.
25. Lombardi, D.; Pant, S. Nonparametric k-nearest-neighbor entropy estimator. *Physical Review E* **2016**, *93*, 013310.
26. Beirlant, J.; Dudewicz, E.J.; Györfi, L.; Van der Meulen, E.C. Nonparametric entropy estimation: An overview. *International Journal of Mathematical and Statistical Sciences* **1997**, *6*, 17–39.
27. Gao, S.; Ver Steeg, G.; Galstyan, A. Efficient estimation of mutual information for strongly dependent variables. *Artificial intelligence and statistics*. PMLR, 2015, pp. 277–286.
28. Benner, P.; Gugercin, S.; Willcox, K. A survey of projection-based model reduction methods for parametric dynamical systems. *SIAM review* **2015**, *57*, 483–531.
29. Benner, P.; Ohlberger, M.; Cohen, A.; Willcox, K. *Model reduction and approximation: theory and algorithms*; SIAM, 2017.
30. Quarteroni, A.; Rozza, G.; others. *Reduced order methods for modeling and computational reduction*; Vol. 9, Springer, 2014.
31. Ma, Y.; Fu, Y. *Manifold learning theory and applications*; CRC press, 2011.
32. Amsallem, D.; Haasdonk, B. PEBL-ROM: Projection-error based local reduced-order models. *Advanced Modeling and Simulation in Engineering Sciences* **2016**, *3*, 1–25.
33. Maday, Y.; Stamm, B. Locally adaptive greedy approximations for anisotropic parameter reduced basis spaces. *SIAM Journal on Scientific Computing* **2013**, *35*, A2417–A2441.